BMC Musculoskeletal Disorders

RESEARCH

Open Access

Exploring the correlation between magnetic resonance diffusion tensor imaging (DTI) parameters and aquaporin expression and biochemical composition content in degenerative intervertebral disc nucleus pulposus tissue: a clinical experimental study

Shuang Chen[1†], Shenglu Sun[1†], Nan Wang[1], Xiaoyang Fang[1], Lin Xie[1,2*], Fei Hu[3*] and Zhipeng Xi[1,3*]

Abstract

Objective This study investigates the correlation between magnetic resonance diffusion tensor imaging (DTI) parameters and biochemical composition in degenerative intervertebral disc nucleus pulposus tissue, offering a potential reference for the clinical diagnosis and efficacy evaluation of intervertebral disc degeneration.

Methods Human lumbar intervertebral disc nucleus pulposus tissue samples were collected *via* full endoscopic minimally invasive surgery. DTI was employed to quantitatively measure fractional anisotropy (FA) and apparent diffusion coefficient (ADC) values in the degenerative nucleus pulposus, examining the relationship between Pfirrmann grading and these DTI parameters. Western blotting was used to detect the expression levels of aquaporin 1 (AQP1) and aquaporin 3 (AQP3) in the degenerative tissue. The glycosaminoglycan (GAG) content was quantified using the dimethylmethylene blue (DMMB) colorimetric assay, and collagen content was assessed with the Sircol soluble collagen assay kit. The relationship between Pfirrmann grading and biochemical composition was also analyzed. Finally, correlation analysis was performed between the FA and ADC values from the human nucleus pulposus tissue and their GAG and collagen contents.

Results A total of 39 patients (19 males, 20 females) with lumbar disc herniation (LDH), averaging 54.41 years of age, were included. As the degree of Pfirrmann degeneration increased, FA values rose, while ADC values continuously declined. Concurrently, as degeneration progressed, expression of AQP1 and AQP3 proteins decreased, GAG content significantly diminished, and collagen content increased. FA values exhibited a moderate negative correlation

†Shuang Chen and Shenglu Sun contributed equally to this work and should be considered co-first authors.

*Correspondence:
Lin Xie
xielin6508@163.com
Fei Hu
18999583620@163.com
Zhipeng Xi
xizhipeng1985@163.com
Full list of author information is available at the end of the article

with GAG content (r = -0.5974, $P < 0.0001$) and a strong positive correlation with collagen content ($r = 0.8694$, $P < 0.0001$). ADC values showed a moderate positive correlation with GAG content ($r = 0.6873$, $P < 0.0001$) and a strong negative correlation with collagen content (r = -0.8502, $P < 0.0001$).

Conclusion The FA and ADC values derived from magnetic resonance DTI, along with the protein expression levels of AQPs, can reflect the severity of intervertebral disc degeneration to a certain extent. Additionally, the content of glycosaminoglycans and collagen in the nucleus pulposus of the intervertebral disc correlates with the FA and ADC values of the DTI parameters. Therefore, magnetic resonance DTI quantitative imaging provides a means to assess the biochemical composition changes within the intervertebral discs, offering valuable insights for the clinical diagnosis and evaluation of therapeutic efficacy in intervertebral disc degenerative diseases.

Trial registration Chinese Clinical Trial Registry, ChiCTR2000041151, Registered on 19 December, 2020, https://www.chictr.org.cn/showproj.html?proj=206119.

Keywords Intervertebral disc degeneration (IDD), Diffusion tensor imaging (DTI), Aquaporins, Glycosaminoglycan content, Collagen content

Introduction

Low back pain is a prevalent musculoskeletal disorder worldwide, with approximately 80% of individuals experiencing acute or chronic episodes during their lifetime. Epidemiological studies indicate that low back pain affects approximately 630 million people globally, with its incidence and associated treatment costs ranking among the highest worldwide [1]. Additionally, as the global population ages, low back pain resulting from intervertebral disc degenerative disease has become a major factor impacting the quality of life for middle-aged and elderly individuals, placing a substantial economic burden on society [2]. Chronic low back pain is now recognized as a global health threat, underscoring the importance of enhancing prevention and treatment strategies for this condition. Intervertebral disc degeneration (IDD) is a key pathological mechanism underlying this disorder. The intervertebral disc is primarily composed of the nucleus pulposus, annulus fibrosus, and cartilage endplate, with its principal constituents being collagen, proteoglycan, and water. Abnormal changes in the biochemical composition of the intervertebral disc—such as alterations in matrix macromolecules like proteoglycans and collagen—can modify the disc's material properties, leading to biomechanical imbalances and subsequent degenerative changes [3, 4]. It is clear that alterations in the biochemical composition of the intervertebral disc serve as the initiating factors for IDD. Studies suggest that signs of IDD are present in most individuals over the age of 30, although these may not manifest as symptoms such as low back pain. Degeneration progressively worsens with age [5, 6]. Therefore, early diagnosis of IDD is of significant clinical importance for the reconstruction and regeneration of degenerated intervertebral disc tissue.

Aquaporins (AQPs) are hydrophobic, small molecule transmembrane proteins found throughout mammals, involved in the transport of water and solutes, and are essential for the proper function of various organ systems and cell types [7]. The nucleus pulposus of the human intervertebral disc is a highly permeable gelatinous tissue, which adapts to vertical stress primarily by regulating water content. Its nutrient transport is also dependent on the rapid movement of water molecules [8]. Recent research has demonstrated the expression of AQPs in nucleus pulposus tissues [9]. Aquaporin 1 (AQP1), found in red blood cells, vascular endothelium, sweat glands, and lungs, exhibits notable oxygen permeability. Under hypoxic conditions, upregulation of AQP1 expression facilitates the transmembrane transport of oxygen molecules, thereby mitigating hypoxic injury [10]. Some studies suggest that the expression of AQP1 gradually decreases as intervertebral discs age [11]. Similarly, AQP3 is a transmembrane transport protein responsible for transporting water molecules across osmotic pressure gradients in cell membranes [12]. AQP3 expression has been shown to be significantly lower in the nucleus pulposus cells of degenerated human intervertebral discs compared to those in normal intervertebral discs [13]. Consequently, AQP1 and AQP3 play critical roles in the nutrient supply and transport of metabolic substances within medullary tissues.

Conventional Magnetic Resonance Imaging (MRI) evaluates IDD qualitatively using sequences such as T2-weighted imaging (T2WI) and T1-weighted imaging (T1WI), which detect changes in signal intensity and morphology within the disc. However, these sequences are limited to identifying late-stage disc alterations, showing low sensitivity to early degenerative changes and failing to accurately quantify the degree of degeneration [14]. The Pfirrmann classification system, currently the most widely used visual grading method in clinical practice, is primarily concerned with morphological

assessments of degenerated intervertebral discs. This system struggles to precisely quantify degeneration severity and is not sensitive to early stages of the condition [15]. In contrast, Diffusion Tensor Imaging (DTI) has the ability to quantitatively assess tissue microstructural characteristics and evaluate the extent of neural injury, making it a powerful complement to standard MRI procedures [16]. Encouragingly, growing research is highlighting the significant potential of DTI in evaluating lumbar degenerative disorders and spinal nerve injuries, suggesting that DTI could play a critical role in enhancing our understanding and management of these conditions [17–19]. DTI is a non-invasive imaging technique that provides a three-dimensional view of tissue microstructure, offering a more detailed assessment of intervertebral disc lesions. Its primary quantitative parameters, Fractional Anisotropy (FA) and Apparent Diffusion Coefficient (ADC), measure the speed and direction of water molecule diffusion, reflecting the microstructure and functional status of the intervertebral disc [20]. Notably, FA and ADC values can quantify microstructural changes in compressed nerve roots caused by lumbar disc herniation (LDH). Studies have demonstrated that a decrease in FA values indicates tissue damage, demyelination, and axonal injury in compressed nerve roots, while an increase in ADC values correlates with inflammatory responses and tissue edema [19]. Given these findings, this study explores the correlation between DTI parameters (FA and ADC values) and the expression of AQPs in degenerating medullary tissues.

In previous research, a bibliometric analysis of quantitative MRI techniques in IDD was conducted, concluding that DTI fiber tractography can quantitatively assess nerve root lesions, and its parameters can reveal microstructural changes in intervertebral disc tissues. This represents a growing research trend [21]. Therefore, the objective of this study is to employ magnetic resonance DTI quantitative imaging to noninvasively evaluate the biochemical composition within the intervertebral disc and provide a foundation for early quantitative diagnosis of IDD.

Materials

Experimental materials

Source and grouping of cases

Patients diagnosed with LDH and admitted to the Department of Orthopedics at Nanjing University of Traditional Chinese and Western Medicine Affiliated Hospital for minimally invasive surgery between November 2021 and November 2023 were enrolled in this study. This represents a secondary analysis of a single-center prospective study on quantitative MRI and aquaporin correlation in spinal degenerative diseases, which is registered with the China Clinical Trial Registry (chictr.org.cn) (registration number: ChiCTR2000041151). To ensure the study's protocol was comprehensive, it was additionally approved by our Ethics Committee (Ethics No. 2023-LWKYZ-085).

All participants voluntarily enrolled in the study and provided written informed consent. According to the Pfirrmann grading system [15], and based on sagittal T2-weighted imaging (T2WI) images, two experienced spinal surgeons independently classified the discs into four groups: group A (grade II), group B (grade III), group C (grade IV), and group D (grade V). In case of discrepancies, the two surgeons consulted and resolved the differences through discussion.

Case selection

Inclusion criteria were as follows: Patients diagnosed with LDH, unresponsive to at least 3 months of conservative treatment, and requiring total endoscopic lumbar disc nucleus pulposus removal surgery, performed by the same chief surgeon. MRI and DTI were conducted prior to surgery, and patients had complete medical records. Participants also showed good adherence to the study protocol, voluntarily accepted the terms of the study, and signed the informed consent form.

Exclusion criteria were as follows: Patients with distorted or low-quality MRI and DTI images that significantly impacted data measurement; those with conditions such as scoliosis, spinal tumors, infections, tuberculosis, or other metabolic wasting diseases.

Processing of human lumbar disc nucleus pulposus tissue samples

The experimental material consisted of human lumbar disc nucleus pulposus tissue excised during surgery. The procedure involved careful removal of soft tissue from the surface of the ligamentum flavum *via* endoscopy. The ligamentum flavum was then incised to expose the dural structure, and the dura mater was gently displaced to protect the nerve root. After penetrating the annulus fibrosus, the loose nucleus pulposus tissue was extracted from within the annulus breach. Immediately following extraction, the tissue was rinsed repeatedly with a tissue balancing solution, transported to the laboratory in a liquid nitrogen tank, and processed under sterile conditions. Within 1 h in a sterile ultra-clean bench, bone-like tissue was discarded, and the nucleus pulposus was separated, placed into a freezing tube, and stored at −80 °C for further analysis.

Experimental reagents

The following reagents were utilized in the study: AQP1 antibody (bs-1506R, Bioss, China), AQP3 antibody

(bs-1253R, Bioss, China), GAPDH antibody (ab181602, Abcam, USA), goat anti-rabbit IgG secondary antibody (ab205718, Abcam, USA), Western primary antibody dilution (P0023A, Beyotime, China), QuickBlockTM Western blocking solution (P0252, Beyotime, China), Western rapid membrane transfer solution (10 ×) (P0572, Beyotime, China), SDS-PAGE protein loading buffer (5 ×, odorless) (P0286, Beyotime, China), BCA protein quantification kit (P0010S, Beyotime, China), One Step PAGE Gel Fast Preparation Kit (E303-01, Vazyme, China), Enhanced ECL Electrochemiluminescence Reagent (BL520A, Biosharp, China), Tissue Glycosaminoglycan (GAG) Total Content Dimethyl Methylene Blue (DMMB) Colorimetric Quantitative Detection Reagent (JM7861, Yuduobio, China), Sircol soluble collagen assay kit (S1000, Biocolor, UK), glacial acetic acid (A801296, Macklin, China), gastric protease (p6887, Sigma-Aldrich, Germany).

Experimental instruments

Instruments used included a three-dimensional frozen grinding instrument (JXCL-3 K, Jingxin, China), constant temperature water bath (TSGP05, Thermo, USA), high-speed low-temperature centrifuge (5424R, Eppendorf, Germany), vertical electrophoresis instrument (PowerPac Basic, Bio-Rad, USA), universal protein transfer system (Trans-Blot Turbo, Bio-Rad, USA), automatic full-wavelength enzyme standard instrument (Infinite M200Pro, Tecan, Switzerland), automatic chemiluminescence image analysis system (5200, Tanon, China), and a 3.0T magnetic resonance imager (MR750, GE Discovery, USA).

Experimental methods

MRI and DTI examinations

All patients in this study underwent preoperative lumbar quantitative magnetic resonance imaging using a multi-transmission scanner system equipped with a dedicated 8-channel spinal coil (MR750, GE Discovery, USA). The scanning parameters are provided in Table 1.

Table 1 Magnetic resonance Imaging parameters

Parameters	T2-weighted image	DTI
Plane	Sagittal	Axial
Scan time	1 min 14s	5 min 09s
Sequences	Fast spin echo (FSE)	Single shot echo planar imaging (ssEPI)
Repetition time, ms	2300	6000
Echo time, ms	105	76
Matrix	320 × 224	256 × 256
Bandwidth	160 Hz/Rx	1953 Hz/Rx
Field of view, mm	280 × 280	250 × 250
Slice thickness, mm	4	3
Interslice gap, mm	1	0.5
No.slices	13	19

DTI image processing and parameter measurement

The original DTI data were processed using qMRLAB 2.4.2 software to generate pseudo-colored images for FA and ADC of the intervertebral discs. FA and ADC values of the nucleus pulposus were measured at the central cross-section of the disc to define regions of interest (ROI) for both FA and ADC. The ROIs were delineated by an associate chief radiologist with extensive experience and an associate chief spinal surgeon with three years of specialized training. In case of discrepancies, the two experts consulted to resolve any differences by consensus. The methodology employed is as follows [22]: On the first echo T2WI image, the length of the anterior-posterior diameter of the disc was measured and divided in a 1:3:1 ratio [23, 24]. Rectangular boxes were manually drawn in the anterior and posterior regions of the central nucleus pulposus, with a length of 1 cm and a width equal to 1/5 of the anteroposterior diameter of the disc. A circle, with a diameter corresponding to 3/5 of the anterior-posterior length of the disc, was drawn around the remaining central nucleus pulposus. These ROIs were then transferred to the DTI image by copying and pasting. Each nucleus pulposus was measured three times, and the average value was used [25].

Western blotting experiment to detect the expression of AQP1 and AQP3 proteins

The experiment was organized into four groups: A, B, C, and D. Nucleus pulposus samples were retrieved from a −80 °C freezer and carefully dissected into distinct tissue types: nucleus pulposus, annulus fibrosus, and ligament tissue. A 40 mg sample of nucleus pulposus was accurately weighed, minced, and placed into a pre-chilled EP tube. To each tube, 800 μL of pre-chilled RIPA lysis buffer and 2–3 grinding beads were added. The samples were then homogenized in a mill at −30 °C until no visible solid remains (12,000 rpm for 15 min), and the supernatant was collected. Protein concentration was determined using a BCA protein quantification kit. For each group, 200 μL of protein was taken, mixed with 5× SDS loading buffer, and boiled for 5 min to denature the proteins. The gel was prepared according to the One-Step PAGE Gel Fast Preparation Kit instructions, tightly clamped, and placed in the electrophoresis tank. After loading, electrophoresis was performed, followed by membrane transfer. The membrane was placed in a dish containing a blocking solution and agitated at room temperature for

20 min. Primary antibodies—AQP1 (1:1000, bs-1506R, Bioss, China), AQP3 (1:1000, bs-1253R, Bioss, China), and GAPDH (1:10000, ab181602, Abcam, USA)—were added, and incubation occurred overnight at 4 °C on a shaker. After three washes with TBST at room temperature (5 min each), the secondary antibody (1:2000, ab205718, Abcam, USA) was added, followed by a 1-hour incubation at room temperature on a shaker. Following three additional washes with TBST, chemiluminescence detection was performed using ECL, and the results were visualized and photographed with a chemiluminescence image analysis system. The statistical analysis was based on the grayscale ratios of AQP1/GAPDH and AQP3/GAPDH.

Dimethylmethylene blue (DMMB) colorimetric method for measuring glycosaminoglycan content in nucleus pulposus tissue

Nucleus pulposus tissue (200 mg) was accurately weighed, and 3 mL of Reagent A was added for cleaning. The specimen was transferred to a liquid nitrogen tank overnight. The following day, the cryovial was removed, and the tissue was immediately crushed into powder using a grinding rod, ensuring minimal freezing and thawing during the grinding process. The tissue was then placed into a 1.5 mL centrifuge tube, and 500 μL of Reagent B was added. The mixture was vortexed vigorously for 1 min and then incubated in a 56 °C water bath for 16 h, followed by a 10-minute incubation at 90 °C. Afterward, the sample was centrifuged at 13,000 rpm for 15 min in a high-temperature, low-speed centrifuge, and the supernatant was collected. Standard samples were prepared according to the instructions, and a standard curve was constructed. To analyze the sample, 50 μL of the specimen was taken, 1 mL of Reagent C was added, and the mixture was vortexed for 15 s. It was incubated in the dark at room temperature for 30 min, with vortexing every 5 min. After the incubation, the sample was centrifuged at 13,000 rpm for 15 min, and the supernatant was discarded. Then, 1 mL of Reagent D was added to the test tube, vortexed for 15 s, and incubated in the dark at room temperature for 5 min. The mixture was transferred to a 96-well plate, with three replicate wells per group. The OD value was measured at 656 nm using an enzyme-linked immunosorbent assay (ELISA) reader. The glycosaminoglycan content of the sample was determined from the standard curve, and the concentration was calculated.

Sircol soluble collagen assay to measure collagen content

Human nucleus pulposus tissue (50 mg) was accurately weighed and incubated in 1 mL of 0.5 mol/L glacial acetic acid and 0.1 mg/mL pepsin on a shaking incubator at 4 °C for 24 h. Following the protocol, collagen was separated and concentrated, preparing the sample for testing. Three groups were prepared: blank (100 μL deionized water), standard (0, 15, 25, and 50 μg standard products in 100 μL deionized water), and sample (100 μL test sample). Sircol dye reagent (1.0 mL) was added to each test tube, and the mixture was shaken for 30 min. It was centrifuged at 13,000 rpm for 15 min, and the supernatant was discarded. Then, 750 μL of ice-cold acid-salt wash reagent was added to the centrifuge tube, and the mixture was shaken and centrifuged again at 13,000 rpm for 5 min, with the supernatant discarded. Alkaline reagent (1.0 mL) was added to the blank, standard, and sample groups, and the mixture was vortexed for 10 min. Each group of samples was transferred to a 96-well plate, with 200 μL per well and three replicate wells per group. The OD value was measured at 556 nm using an ELISA reader. The soluble collagen content was calculated from the standard curve, and the concentration was determined.

Statistical methods

Data analysis was conducted using IBM SPSS Statistics version 25.0 (IBM Corp., Armonk, NY, USA) and GraphPad Prism software version 9.5.1 (San Diego, CA, USA). For normally distributed data, one-way analysis of variance (ANOVA) was used to assess variance homogeneity across groups, and the Kruskal-Wallis test was applied for heterogeneity of variance. Measurement data were presented as mean ± standard deviation ($\bar{X} \pm$ SD). For non-normally distributed data, the Wilcoxon rank sum test was used. Correlation analysis was performed using Pearson's product-moment correlation coefficient. Statistical significance was set at $P < 0.05$.

Results

General characteristics of the research object

A total of 39 patients with LDH participated in this study, including 19 males and 20 females. The mean age was 54.41 years (SD = 14.99 years). According to the Pfirrmann grading system, the distribution of disc grades was as follows: 9 grade II discs, 10 grade III discs, 10 grade IV discs, and 10 grade V discs, as detailed in Table 2 and Table S1.

Western blotting experiment to detect the expression of AQP1 and AQP3 proteins in nucleus pulposus tissue

The results of the Western blotting experiment demonstrated that, compared to group A, protein expressions of AQP1 and AQP3 were significantly reduced in groups B, C, and D ($P < 0.05$). Additionally, protein expressions of AQP1 and AQP3 were significantly lower in groups C and D compared to group B ($P < 0.05$). No statistically

Table 2 General information of the participants

Number of cases	39 cases
Gender *n* (%)	
Male	19 cases (48.72%)
Female	20 cases (51.28%)
Age	54.41 ± 14.99 years
Diagnosis	
Lumbar Disc Herniation	35 cases (89.74%)
Lumbar Disc Herniation with Spinal Stenosis	4 cases (10.26%)
Direction of Disc Herniation	
Left side	23 segments (58.97%)
Right side	16 segments (41.03%)
Disc Herniation Level	
L2/3	1 segment (2.56%)
L3/4	2 segments (5.13%)
L4/5	24 segments (61.54%)
L5/S1	12 segments (30.77%)
Pfirrmann grading	
Grade II	9 discs (23.08%)
Grade III	10 discs (25.64%)
Grade IV	10 discs (25.64%)
Grade V	10 discs (25.64%)

significant difference in the expressions of AQP1 and AQP3 was observed between groups C and D ($P > 0.05$), as shown in Fig. 1. These results suggest that with increasing degeneration of human nucleus pulposus tissue, water content decreases, leading to a gradual reduction in AQP1 and AQP3 protein levels.

Contents of glycosaminoglycan and collagen in nucleus pulposus tissues with different Pfirrmann degeneration grades

The glycosaminoglycan standard curve equation was $Y = 0.1192X + 0.1397$ ($R^2 = 0.9393$). The DMMB assay results revealed that the concentration of glycosaminoglycans in group A was 89.80 ± 7.68 μg/mL, in group B was 78.46 ± 8.95 μg/mL, in group C was 60.79 ± 8.61 μg/mL, and in group D was 43.37 ± 9.92 μg/mL. Statistically significant differences were observed among all groups ($P < 0.05$). The collagen standard curve equation was $Y = 0.01599X - 0.003289$ ($R^2 = 0.9797$). The Sircol soluble collagen assay indicated a significant increase in collagen content in the nucleus pulposus as the Pfirrmann grade progressed ($P < 0.05$), as shown in Fig. 2.

FA and ADC values of nucleus pulposus tissues with different Pfirrmann degeneration grades

DTI scanning results indicated that the reference range for FA values in nucleus pulposus was 0–0.4 (10^{-3} mm^2/s). No statistically significant difference was found between groups C and D ($P > 0.05$), but significant differences were observed in comparisons among the other groups ($P < 0.05$). Similarly, the reference range for ADC values in nucleus pulposus was 1.2–2.2 (10^{-3} mm^2/s), with no significant difference between groups C and D ($P > 0.05$), while significant differences were found between other groups ($P < 0.05$). As shown in Table 3; Fig. 3, as the degree of degeneration of the human the nucleus pulposus increased, FA values rose, while ADC values continuously decreased.

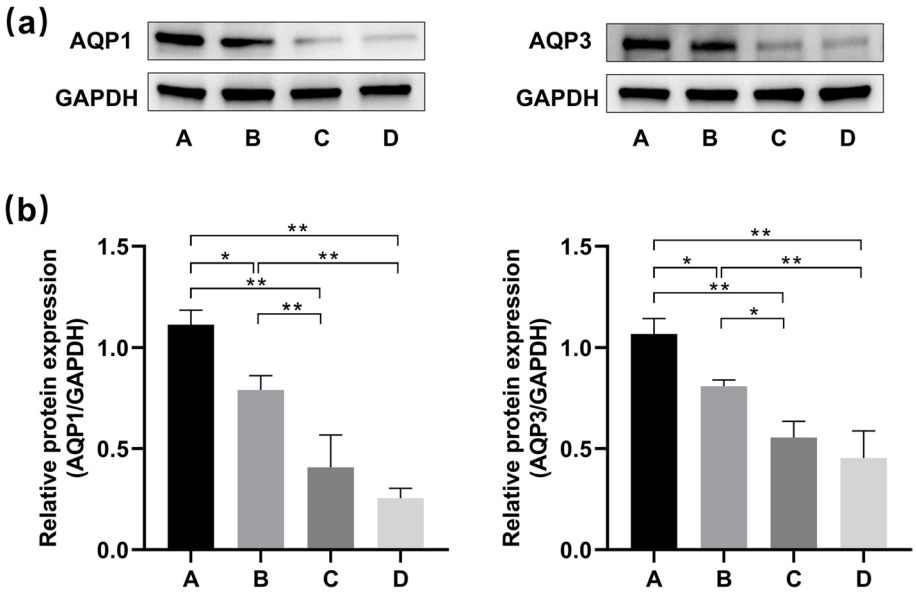

Fig. 1 Expression of AQP1 and AQP3 proteins in degenerated nucleus pulposus tissues of each group. *, $P < 0.05$; **, $P < 0.01$. AQP1, Aquaporin 1; AQP3, Aquaporin 3

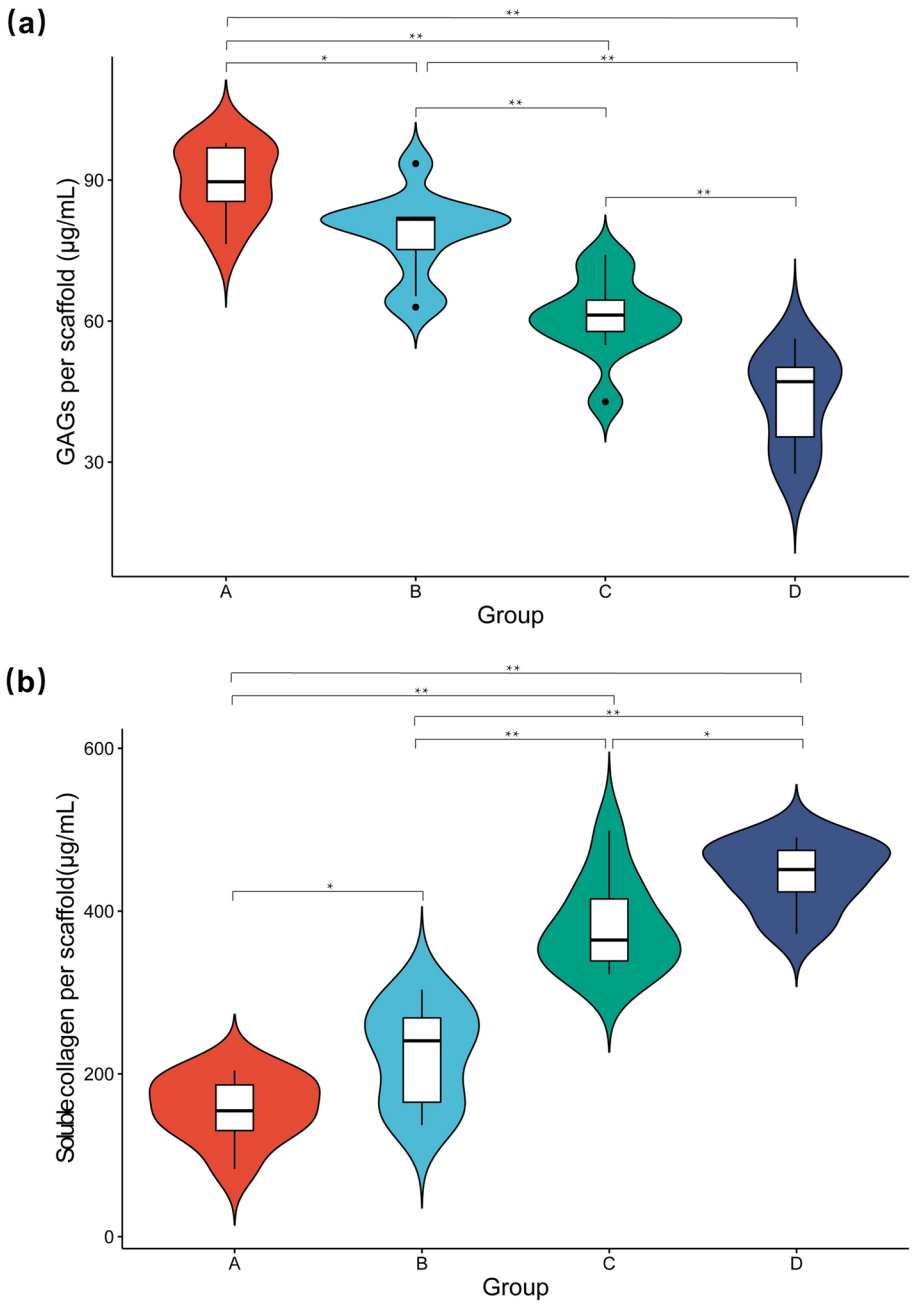

Fig. 2 Contents of glycosaminoglycan and collagen in nucleus pulposus tissues with different Pfirrmann degeneration grades. *, $P < 0.05$; **, $P < 0.01$. GAG, Glycosaminoglycan

Correlation analysis between FA and ADC values and glycosaminoglycan and collagen content in human degenerative nucleus pulposus tissue

A correlation analysis was performed between the FA and ADC values obtained from human nucleus pulposus tissue and its GAG and collagen content. The results indicated that the FA value of nucleus pulposus DTI exhibited a moderate negative correlation with its GAG content ($r = -0.5974$, $P < 0.0001$) and a strong positive correlation with its collagen content ($r = 0.8694$, $P < 0.0001$). Additionally, the ADC value showed a moderate positive correlation with GAG content ($r = 0.6873$, $P < 0.0001$) and a strong negative correlation with collagen content ($r = -0.8502$, $P < 0.0001$) (Fig. 4).

Discussion

IDD is widely recognized as the primary cause of degenerative disc diseases, which can lead to complications such as disc herniation, spondylolisthesis, osteophytic

Table 3 FA and ADC values of nucleus pulposus tissues at different Pfirrmann degeneration grades

Group	FA value ($10^{-3}mm^2/s$)	ADC value ($10^{-3}mm^2/s$)
A (Grade II)	0.0939 ± 0.0069	2.0016 ± 0.089
B (Grade III)	0.1530 ± 0.0048	1.8542 ± 0.1395
C (Grade IV)	0.2100 ± 0.0114	1.6389 ± 0.0247
D (Grade V)	0.2601 ± 0.0862	1.5187 ± 0.1627
H value	31.975[a]	28.620[a]
P value	< 0.001	< 0.001

FA Fractional anisotropy, *ADC* Apparent diffusion coefficient

[a] The inter-group data followed a normal distribution with unequal variance, and the Kruskal-Wallis test was used for statistical analysis

hyperplasia, spinal instability, and, in advanced stages, lower limb muscle dysfunction. The current understanding of the pathomechanisms underlying IDD, as explored by scholars both domestically and internationally, can be categorized into three primary theories: (1) Mechanical compression theory: The protruding nucleus pulposus exerts pressure on nerve roots, causing mechanical stimulation, which in turn results in acute back and leg pain. The severity of the pain correlates positively with the extent of nucleus pulposus compression [26]. (2) Chemical inflammation theory: The protruding nucleus pulposus can act as an inflammatory trigger, inducing inflammatory responses in the nerve roots and surrounding tissues. This response increases the sensitivity of dorsal root neurons to mechanical stimuli, exacerbating the pain and discomfort associated with disc degeneration [27]. (3) Autoimmune theory: During the process of IDD, proteoglycans and collagen are released from the protruding intervertebral disc. The body's immune system mistakenly recognizes these substances as foreign antigens, triggering an autoimmune response that intensifies local inflammation [28]. Early diagnosis of disc degeneration is essential for effective management and treatment of degenerative disc diseases.

The nucleus pulposus (NP) tissue is known for its high content of negatively charged glycosaminoglycans and its strong hydrophilic properties. Prolonged physical labor and static postures that place axial stresses on the spine can disrupt the free flow of water molecules into and out of the NP tissue. This disruption causes the osmolarity of the NP tissue to become significantly higher than that of other extracellular fluids in the body [29]. Furthermore, metabolites within the disc matrix respond to osmotic pressure and concentration gradients primarily through molecular diffusion. These metabolic responses are also influenced by changes in NP volume due to disc activity, and as such, diffusion changes are considered an early sign of disc degeneration [30]. Biochemical changes within the intervertebral disc, such as the loss of collagen and proteoglycans, result in metabolic imbalances within the nucleus pulposus. These imbalances contribute to the degenerative process of the disc. Although these changes do not immediately result in significant structural alterations, they are recognized as early indicators of degeneration [31]. Notably, under conditions of heightened stress, the production of pro-inflammatory cytokines (such as interleukin-1 (IL-1)) increases within the intervertebral disc tissues. This disrupts the glycosaminoglycans in the NP, leading to the degradation of the extracellular matrix and stimulating further inflammatory responses [32]. Consequently, these biochemical changes lead to a reduction in the osmolarity of the NP, further promoting the loss of disc water content. Thus, changes in the osmotic pressure within the intervertebral disc play a pivotal role in the early diagnosis of intervertebral disc degeneration.

AQP proteins are transmembrane water channel proteins that regulate cellular permeability to water and other small molecules. Previous studies have shown that the expression of AQPs in intervertebral disc cells is influenced by the osmotic environment and decreases with disc degeneration [13]. Wang et al. [33] demonstrated that the expression of AQP1 was significantly reduced in the lumbar nucleus pulposus cells of elderly rabbits. They further found that the expression of AQP1 is influenced by extracellular osmotic pressure and oxygen concentration. Specifically, a decrease in the osmotic pressure of the cellular environment leads to the downregulation of AQP1 expression, while a decrease in oxygen concentration results in its upregulation. Tas et al. [34] confirmed through immunohistochemical staining that the expressions of AQP1 and AQP3 in the intervertebral discs of rats gradually decreased with the progression of IDD. In 2-month-old rats, AQP1 and AQP3 are primarily localized in the inner layer of the nucleus pulposus and annulus fibrosus, with weak immunostaining observed in the outer annular region. However, by 18 months of age, the number of AQP1 and AQP3-positive cells in the intervertebral disc was significantly reduced. Xie et al. [35] identified a correlation between IDD and AQP3 expression in human nucleus pulposus cells. Overexpression of AQP3 was found to inhibit the Wnt/β-catenin signaling pathway, promote the proliferation of human nucleus pulposus cells, significantly inhibit extracellular matrix degradation, and delay the progression of IDD. These findings suggest that AQP1 and AQP3 play critical roles in the supply of nutrients and the transport of metabolic substances within the nucleus pulposus.

DTI technology is based on diffusion-weighted imaging, which utilizes the diffusion of water molecules in various tissues to reflect the microstructural characteristics of those tissues. DTI quantifies these characteristics

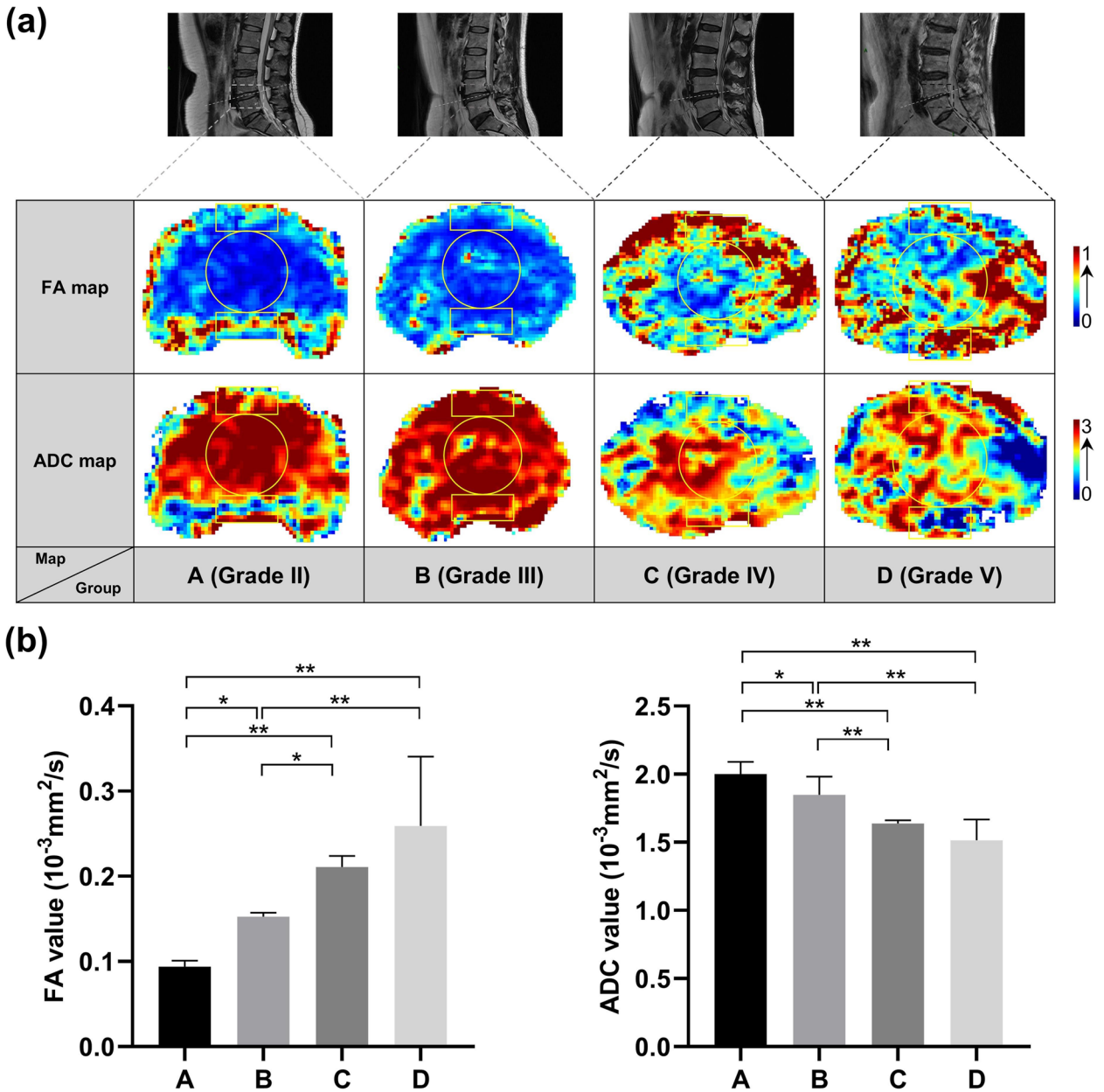

Fig. 3 FA and ADC values of nucleus pulposus tissues at different Pfirrmann degeneration grades. **a** DTI pseudo-color images of degenerated nucleus pulposus in each group. **b** FA and ADC values of degenerated nucleus pulposus in each group. *, $P < 0.05$; **, $P < 0.01$. FA, Fractional anisotropy; ADC, Apparent diffusion coefficient; DTI, Diffusion tensor imaging

using parameters such as the FA value and the ADC value. In tissues with well-ordered structures, the diffusion of water molecules typically occurs in a specific direction. The FA value describes the directional preference of water molecule diffusion, while the ADC value reflects the extent of water diffusion motion. Although DTI was initially developed for parenchymal nerve tract imaging, its application has expanded far beyond the central nervous system [36, 37]. In recent years, the application of DTI in the study of degenerative disc diseases has increased [38, 39]. Dan et al. [40] conducted a macroscopic experimental study using DTI and fiber tractography to reconstruct the three-dimensional microstructure of the annulus fibrosus. The results revealed significant structural differences in the anisotropic properties between lamellae along the width of the fiber bands. The outer lamellar structures were found to provide essential support for motion and

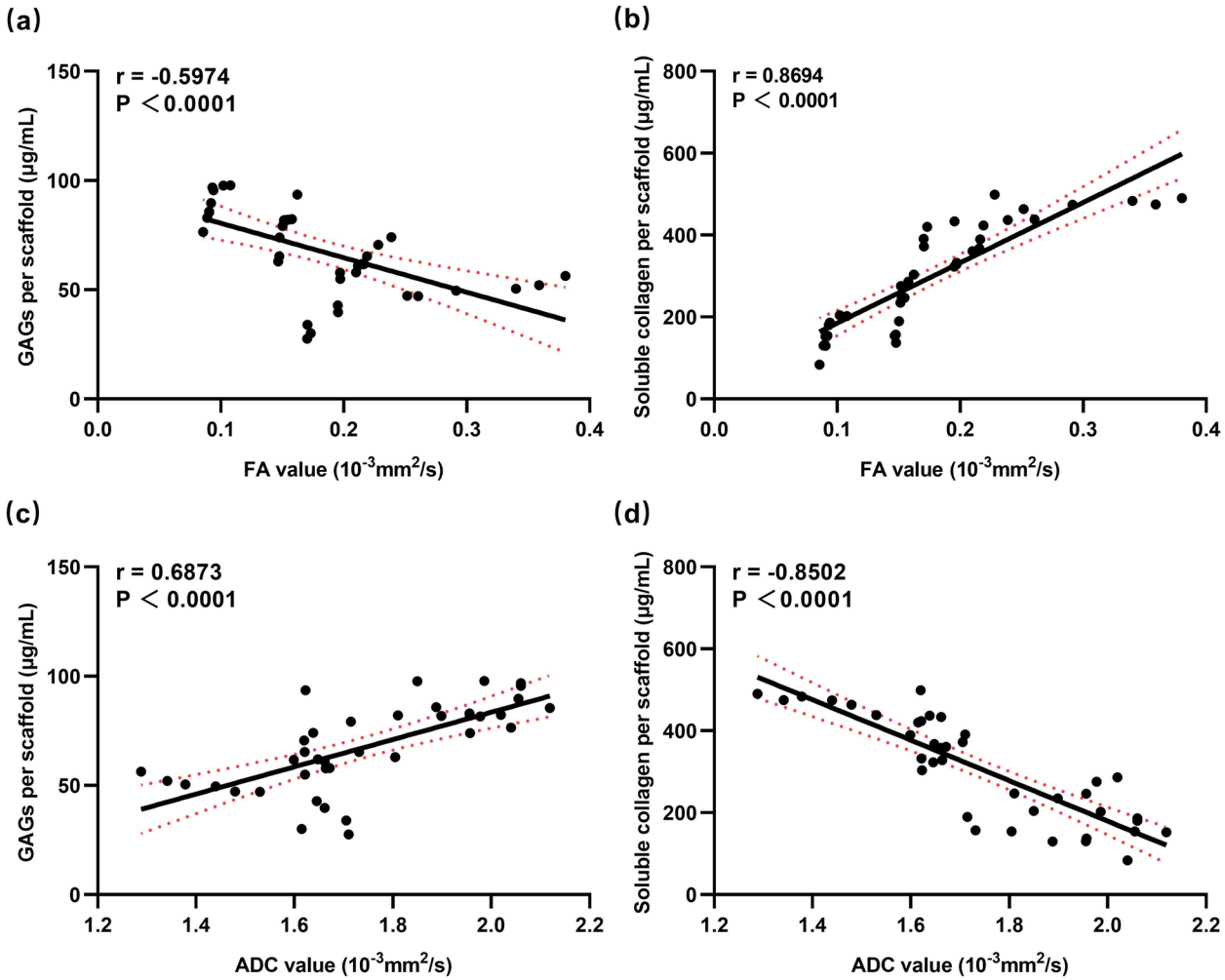

Fig. 4 Correlation analysis between FA, ADC values and glycosaminoglycan, collagen content in human degenerative nucleus pulposus tissue

nutrition. Notably, both FA and ADC values can reflect the pathophysiological state of nerve fiber bundles affected by LDH [41]. Studies have shown that the FA value in the corresponding segment is usually decreased after disc herniation compresses the nerve [42]. However, whether the ADC value increases following nerve injury remains controversial [43]. Wang et al. [44] conducted a meta-analysis of 369 patients with LDH and found that, compared to the healthy side, the FA value of the compressed nerve root on the affected side was significantly reduced (weighted mean difference = −0.08, 95% confidence interval: −0.09 to −0.07, $P \leq 0.001$, $I^2 = 87.6\%$). In contrast, the ADC value was significantly increased (weighted mean difference = 0.25, 95% confidence interval: 0.20 to 0.30, $P \leq 0.001$, $I^2 = 71.4\%$). Jin et al. [45] retrospectively analyzed DTI parameters in the lumbar intervertebral discs of 41 patients and found that the FA value of the nucleus pulposus was positively correlated with the Pfirrmann grade ($r = 0.67$, $P < 0.01$), while the ADC value of the nucleus pulposus was negatively correlated with the Pfirrmann grade ($r = -0.71$, $P < 0.01$). They also noted that the impact of disc herniation on the signal of the nucleus pulposus was relatively minor. These findings suggest that quantitative evaluation of the degree of degeneration in nucleus pulposus tissue using DTI imaging is feasible, offering a valuable tool for assessing the biochemical components within the nucleus pulposus.

This study included 39 patients with LDH (19 males and 20 females), with a mean age of 54.41 years. Nucleus pulposus tissue was obtained from all patients *via* minimally invasive surgery. DTI of the affected disc segments revealed elevated Pfirrmann classifications, increased degeneration, higher FA values, and lower ADC values of the nucleus pulposus, consistent with previous studies [45]. It has been demonstrated that degeneration of the nucleus pulposus leads to disruption of the collagen fiber network and the layered structure of the peripheral annulus, with peripheral fibers gradually replacing

glycosaminoglycans. This results in the loss of the distinct boundary between the nucleus pulposus and annulus fibrosus, limiting isotropic water diffusion in the nucleus pulposus, which in turn increases FA values. Concurrently, a decrease in water content and glycosaminoglycan levels, along with fiber fusion, restricts water diffusion, leading to a reduction in ADC values [23]. Western blot analysis indicated that as degeneration progressed, the expression of AQP1 and AQP3 proteins in groups A-D progressively decreased, suggesting a potential relationship between AQP expression and IDD. Combined analysis of DMMB and Sircol colorimetry revealed a significant reduction in glycosaminoglycan content and a notable increase in collagen content as the Pfirrmann classification increased ($P<0.05$). These observations suggest that glycosaminoglycan degradation in degenerative nucleus pulposus may trigger a compensatory increase in collagen, due to metabolic imbalance within the extracellular matrix. This disruption blurs the normal boundary between the nucleus pulposus and annulus fibrosus, causing their fusion. Type II collagen from the inner annulus fibrosus may penetrate this boundary into the nucleus pulposus, contributing to increased collagen content, which, in turn, diminishes the nucleus pulposus's material transport efficiency. Correlation analysis of FA and ADC values obtained from DTI of the nucleus pulposus and its glycosaminoglycan and collagen content revealed that the FA value was moderately negatively correlated with glycosaminoglycan content ($r = -0.5974$, $P<0.0001$) and highly positively correlated with collagen content ($r=0.8694$, $P<0.0001$). Additionally, the ADC value showed a moderate positive correlation with glycosaminoglycan content ($r=0.6873$, $P<0.0001$) and a strong negative correlation with collagen content ($r = -0.8502$, $P<0.0001$).

This study has several limitations. First, it is a preliminary exploratory clinical study with a relatively small sample size, and future research will involve larger, multi-center, prospective studies. Second, a slice thickness of 3 mm was used for DTI, which may pose challenges in cases of severe degeneration, where significant disc height collapse occurs. To address this, scans were conducted at the centroid of the sagittal plane of the intervertebral disc, with 3 mm slices above and below this point. Western blotting was employed to measure the relative expression of AQPs, but potential issues with the sensitivity and specificity of histone markers may affect the results. Refining the quantitative indices to be measured will be necessary in future studies. While no significant baseline differences were observed across the data groups, further multifactorial analyses are needed to adjust for other confounding factors that were not considered in the current study.

Conclusion

In summary, DTI parameters and the expression levels of AQP1 and AQP3 can reflect the severity of intervertebral disc degeneration to some extent, with the glycosaminoglycan and collagen content in the nucleus pulposus showing a significant correlation with the DTI parameters FA and ADC. Consequently, magnetic resonance DTI quantitative imaging offers a promising approach to assess biochemical changes in the intervertebral disc, which could provide valuable insights for clinical diagnosis and the evaluation of treatment efficacy in degenerative disc diseases.

Supplementary Information

The online version contains supplementary material available at https://doi.org/10.1186/s12891-025-08382-9.

Supplementary Material 1: Table S1. Comparison of patients' baseline information. Figure S1. Standard curve equations for glycosaminoglycan and collagen content.

Acknowledgements

We sincerely appreciate the support and contributions of our colleagues. We thank Bullet Edits Limited for the linguistic editing and proofreading of the manuscript.

Authors' contributions

SC and SS contributed equally to this work. LX, FH, and ZX were responsible for the concept and design of the study. SC, SS, and NW retrieved and analyzed the data. SC, XF, and NW utilized software to generate the figures. SC and SS wrote and revised the manuscript. All authors were fully engaged in the study and the preparation of the manuscript.

Funding

This study was supported by the Project of the National Clinical Research Base of Traditional Chinese Medicine in Jiangsu Province, China (JD2022SZXMS07), the Scientific Research Project of Jiangsu Provincial Health Commission (M2022095), the Seventh Batch of the National Chinese Medicine Experts' Academic Experience Inheritance Work Project (22QGSC6), and the Yili Prefecture Science and Technology Plan Project (YJC2024A21).

Data availability

The datasets used and/or analysed during the current study are available from the corresponding author on reasonable request.

Declarations

Ethics approval and consent to participate

The authors take full responsibility for all aspects of the work, ensuring that any issues concerning the accuracy or integrity of any part of the research are properly investigated and addressed. The study was conducted in accordance with the Declaration of Helsinki (2013 revision) and approved by the Ethics Committee of the Affiliated Hospital of Nanjing University of Traditional Chinese and Western Medicine (Clinical Trial Number: 2023-LWKYZ-085). Informed written consent was obtained from all participants prior to their involvement in the study. Any details that could potentially reveal the identity of the participants have been omitted.

Consent for publication

Not applicable.

Competing interests

The authors declare no competing interests.

Author details
[1]Department of Spine Surgery, Affiliated Hospital of Integrated Traditional Chinese and Western Medicine, Nanjing University of Chinese Medicine, Nanjing, China. [2]The Third Clinical Medical College, Nanjing University of Chinese Medicine, Nanjing, China. [3]Department of Orthopedics, Traditional Chinese Medicine Hospital of Ili Kazak Autonomous Prefecture, Yining, China.

Received: 13 September 2024 Accepted: 31 January 2025
Published online: 17 February 2025

References

1. Global regional. National incidence, prevalence, and years lived with disability for 328 diseases and injuries for 195 countries, 1990–2016: a systematic analysis for the global burden of Disease Study 2016. Lancet (London England). 2017;390(10100):1211–59.
2. Global regional. National incidence, prevalence, and years lived with disability for 301 acute and chronic diseases and injuries in 188 countries, 1990–2013: a systematic analysis for the global burden of Disease Study 2013. Lancet (London England). 2015;386(9995):743–800.
3. Vergroesen PP, Kingma I, Emanuel KS, Hoogendoorn RJ, Welting TJ, van Royen BJ, van Dieën JH, Smit TH. Mechanics and biology in intervertebral disc degeneration: a vicious circle. Osteoarthr Cartil. 2015;23(7):1057–70.
4. Luo X, Sun K, Zhu J, Wang S, Wang Y, Sun J, Shi J. Analysis of intervertebral disc degeneration in patients with ossification of the posterior longitudinal ligament. Quant Imaging Med Surg. 2022;12(3):1919–28.
5. Romeo V, Covello M, Salvatore E, Parente CA, Abbenante D, Biselli R, Ciriello M, Musolino P, Salvatore M, Cangiano A. High prevalence of spinal magnetic resonance imaging findings in asymptomatic young adults (18–22 yrs) candidate to Air Force Flight. Spine. 2019;44(12):872–8.
6. Silva MJ, Holguin N. Aging aggravates intervertebral disc degeneration by regulating transcription factors toward chondrogenesis. FASEB Journal: Official Publication Federation Am Soc Experimental Biology. 2020;34(2):1970–82.
7. Takata K, Matsuzaki T, Tajika Y. Aquaporins: water channel proteins of the cell membrane. Prog Histochem Cytochem. 2004;39(1):1–83.
8. Luo Z, Wei Z, Zhang G, Chen H, Li L, Kang X. Achilles' Heel-The Significance of Maintaining Microenvironmental Homeostasis in the Nucleus Pulposus for Intervertebral Discs. Int J Mol Sci 2023, 24(23).
9. Zhang X, Lv Z, Wei C. Hypo-osmolality activates Wnt/β-catenin mediated by AQP1 in nucleus pulposus cells degeneration. Cellular and molecular biology (Noisy-le-Grand, France) 2024, 70(1):194–199.
10. Echevarría M, Muñoz-Cabello AM, Sánchez-Silva R, Toledo-Aral JJ, López-Barneo J. Development of cytosolic hypoxia and hypoxia-inducible factor stabilization are facilitated by aquaporin-1 expression. J Biol Chem. 2007;282(41):30207–15.
11. Snuggs JW, Tessier S, Bunning RAB, Shapiro IM, Risbud MV, Le Maitre CL. TonEBP regulates the hyperosmotic expression of aquaporin 1 and 5 in the intervertebral disc. Sci Rep. 2021;11(1):3164.
12. Hara-Chikuma M, Satooka H, Watanabe S, Honda T, Miyachi Y, Watanabe T, Verkman AS. Aquaporin-3-mediated hydrogen peroxide transport is required for NF-κB signalling in keratinocytes and development of psoriasis. Nat Commun. 2015;6:7454.
13. Zhang Z, Zhao C, Zhang R, Wang Y, Hu Y, Zhou Q, Li P. Overexpression of Aquaporin-3 Alleviates Hyperosmolarity-Induced Nucleus Pulposus Cell Apoptosis via Regulating the ERK1/2 Pathway. Pain research & management 2022, 2022:1639560.
14. Wu X, Liu C, Yang S, Shen N, Wang Y, Zhu Y, Guo Z, Yang SY, Xing D, Li H et al. Glycine-Serine-Threonine Metabolic Axis Delays Intervertebral Disc Degeneration through Antioxidant Effects: An Imaging and Metabonomics Study. Oxidative medicine and cellular longevity 2021, 2021:5579736.
15. Pfirrmann CW, Metzdorf A, Zanetti M, Hodler J, Boos N. Magnetic resonance classification of lumbar intervertebral disc degeneration. Spine. 2001;26(17):1873–8.
16. Le Bihan D, Mangin JF, Poupon C, Clark CA, Pappata S, Molko N, Chabriat H. Diffusion tensor imaging: concepts and applications. J Magn Reson Imaging: JMRI. 2001;13(4):534–46.
17. Eguchi Y, Oikawa Y, Suzuki M, Orita S, Yamauchi K, Suzuki M, Aoki Y, Watanabe A, Takahashi K, Ohtori S. Diffusion tensor imaging of radiculopathy in patients with lumbar disc herniation: preliminary results. bone Joint J. 2016;98–b(3):387–94.
18. Shinn RL, Pancotto TE, Stadler KL, Werre SR, Rossmeisl JH. Magnetization transfer and diffusion tensor imaging in dogs with intervertebral disk herniation. J Vet Intern Med. 2020;34(6):2536–44.
19. Wu P, Huang C, Li W, Yuan A, Jin A. Application of Magnetic Resonance Diffusion Tensor Imaging in the Clinical Diagnosis of Disc Herniation after Lumbar Spine Injury. J Healthc Eng 2021, 2021:6610988.
20. Vadapalli R, Mulukutla R, Vadapalli AS, Vedula RR. Quantitative Predictive Imaging Biomarkers of Lumbar Intervertebral Disc Degeneration. Asian Spine J. 2019;13(4):527–34.
21. Chen S, Sun D, Wang N, Fang X, Xi Z, Wang C, Chen H, Xie L. Current status and trends in quantitative MRI study of intervertebral disc degeneration: a bibliometric and clinical study analysis. Quant Imaging Med Surg. 2023;13(5):2953–74.
22. Xi Z, Xie Y, Sun S, Wang N, Chen S, Wang G, Li J. IVD fibrosis and disc collapse comprehensively aggravate vertebral body disuse osteoporosis and zygapophyseal joint osteoarthritis by posteriorly shifting the load transmission pattern. Comput Biol Med. 2024;170:108019.
23. Perri M, D'Elia M, Castorani G, Balzano RF, Pennelli A, Al-Badayneh B, Russo A, Guglielmi G, Popolizio T. Assessment of lumbar disc herniaton using fractional anisotropy in diffusion tensor imaging along with conventional T2-weighted imaging. Neuroradiol J. 2020;33(1):24–31.
24. Shen S, Wang H, Zhang J, Wang F, Liu SR. Diffusion weighted imaging, Diffusion Tensor Imaging, and T2* mapping of lumbar intervertebral disc in young healthy adults. Iran J Radiology: Q J Published Iran Radiological Soc. 2016;13(1):e30069.
25. Shi Y, Zou Y, Feng Y, Dou W, Ding H, Wang C, Zhao F, Shi H. A quantitative and clinical evaluation of nerve roots in lumbosacral radiculopathy using diffusion tensor imaging. Japanese J Radiol. 2020;38(3):222–30.
26. Li Y, Fredrickson V, Resnick DK. How should we grade lumbar disc herniation and nerve root compression? A systematic review. Clin Orthop Relat Res. 2015;473(6):1896–902.
27. Cosamalón-Gan I, Cosamalón-Gan T, Mattos-Piaggio G, Villar-Suárez V, García-Cosamalón J. Vega-Álvarez JA: inflammation in the intervertebral disc herniation. Neurocirugia (English Edition). 2021;32(1):21–35.
28. Di Martino A, Merlini L, Faldini C. Autoimmunity in intervertebral disc herniation: from bench to bedside. Expert Opin Ther Targets. 2013;17(12):1461–70.
29. Li P, Gan Y, Xu Y, Li S, Song L, Li S, Li H, Zhou Q. Osmolarity affects matrix synthesis in the nucleus pulposus associated with the involvement of MAPK pathways: a study of ex vivo disc organ culture system. J Orthop Research: Official Publication Orthop Res Soc. 2016;34(6):1092–100.
30. Sood A, Mishra GV, Suryadevara M, Parihar P, Khandelwal S, Manuja N, Saboo K, Shelar SS, Ahuja A, Batra N. Role of Apparent Diffusion Coefficient in evaluating degeneration of the intervertebral disc: a narrative review. Cureus. 2023;15(8):e43340.
31. Melrose J, Guilak F. Diverse and multifunctional roles for perlecan (HSPG2) in repair of the intervertebral disc. JOR Spine. 2024;7(3):e1362.
32. Roberts S, Evans H, Trivedi J, Menage J. Histology and pathology of the human intervertebral disc. J bone Joint Surg Am. volume 2006;88(Suppl 2):10–4.
33. Wang F, Zhu Y. Aquaporin-1: a potential membrane channel for facilitating the adaptability of rabbit nucleus pulposus cells to an extracellular matrix environment. J Orthop Science: Official J Japanese Orthop Association. 2011;16(3):304–12.
34. Taş U, Caylı S, Inanır A, Ozyurt B, Ocaklı S, Karaca Z, Sarsılmaz M. Aquaporin-1 and aquaporin-3 expressions in the intervertebral disc of rats with aging. Balkan Med J. 2012;29(4):349–53.
35. Xie H, Jing Y, Xia J, Wang X, You C, Yan J. Aquaporin 3 protects against lumbar intervertebral disc degeneration via the Wnt/β-catenin pathway. Int J Mol Med. 2016;37(3):859–64.
36. Stein D, Neufeld A, Pasternak O, Graif M, Patish H, Schwimmer E, Ziv E, Assaf Y. Diffusion tensor imaging of the median nerve in healthy and carpal tunnel syndrome subjects. J Magn Reson Imaging: JMRI. 2009;29(3):657–62.
37. Zijta FM, Froeling M, van der Paardt MP, Lakeman MM, Bipat S, van Swijndregt AD, Strijkers GJ, Nederveen AJ, Stoker J. Feasibility of diffusion tensor imaging (DTI) with fibre tractography of the normal female pelvic floor. Eur Radiol. 2011;21(6):1243–9.
38. Wu P, Huang C, Zhao S, Jin A, Shi B. Preoperative quantitative diffusion tensor imaging on the spinal nerve root is a predictor for the surgical outcome of lumbar disc herniation: a prospective study of 117 patients. J Neurosurg Sci. 2023;67(2):219–29.

39. Lian Z, Gao S, Zhang H. Analysis of the curative effect of Diffusion Tensor Imaging-guided percutaneous endoscopic lumbar discectomy. Curr Med Imaging. 2023;19(9):1084–9.
40. Stein D, Assaf Y, Dar G, Cohen H, Slon V, Kedar E, Medlej B, Abbas J, Hay O, Barazany D, et al. 3D virtual reconstruction and quantitative assessment of the human intervertebral disc's annulus fibrosus: a DTI tractography study. Sci Rep. 2021;11(1):6815.
41. Sakai T, Miyagi R, Yamabe E, Fujinaga Y, N NB, Yoshioka H. Diffusion-weighted imaging and diffusion tensor imaging of asymptomatic lumbar disc herniation. J Med Investig. 2014;61(1–2):197–203.
42. Zhang J, Zhang F, Xiao F, Xiong Z, Liu D, Hua T, Indima N, Tang G. Quantitative evaluation of the compressed L5 and S1 nerve roots in unilateral lumbar disc herniation by using Diffusion Tensor Imaging. Clin Neuroradiol. 2018;28(4):529–37.
43. Wu W, Liang J, Ru N, Zhou C, Chen J, Wu Y, Yang Z. Microstructural changes in compressed nerve roots are consistent with clinical symptoms and Symptom Duration in patients with lumbar disc herniation. Spine. 2016;41(11):E661–6.
44. Wang N, Sun D, Zhang X, Xi Z, Li J, Xie L. Nerve abnormalities in lumbar disc herniation: a systematic review and meta-analysis of diffusion tensor imaging. PLoS ONE. 2022;17(12):e0279499.
45. Jin S, Gu X, Li H, Zhu S, Fei J. Quantitative analysis of lumbar disc degeneration by DTI. In: Modern Medical Imaging. vol. 30; 2021: 1004–1006 + 1020.

Publisher's Note